ELSEVIER

Contents lists available at SciVerse ScienceDirect

Surface Science

journal homepage: www.elsevier.com/locate/susc



Water adsorption on SrTiO₃(001): I. Experimental and simulated STM

A.E. Becerra-Toledo a,*, M.R. Castell b, L.D. Marks a

- ^a Department of Materials Science and Engineering, Northwestern University, Evanston, IL 60208, USA
- ^b Department of Materials, University of Oxford, Parks Road, Oxford, OX1 3PH, United Kingdom

ARTICLE INFO

Article history: Received 28 July 2011 Accepted 11 January 2012 Available online 17 January 2012

Keywords:
Strontium titanate
Scanning tunneling microscopy
Density functional theory
Water adsorption
Surface reconstruction
Simulation

ABSTRACT

Density functional theory-based simulations of scanning tunneling micrographs were used for comparison to published experimental images of reconstructed SrTiO $_3$ (001) surfaces. It was found that the addition of dissociatively adsorbed H_2O to the presently accepted structural solution of the 2×1 reconstruction is more consistent with the experimental data. A proposed model for the $c(4\times4)$ reconstruction, based on the hydrated 2×1 structure, agrees well with experiment and is consistent with a formation process consisting of the simple dehydration of a wet 2×1 structure.

© 2012 Elsevier B.V. All rights reserved.

1. Introduction

Strontium titanate, SrTiO₃, is the archetypal perovskite oxide and has a potential use in numerous applications, ranging from thin film growth [1] to heterogeneous catalysis [2]. Moreover, it has emerged as a cornerstone of the novel field of oxide-based electronics, with its UHV-cleaved surface found to form a 2-dimensional electron gas [3]. The performance of strontium titanate in these applications critically depends on its surface structure.

Despite numerous studies, the nature of the stable $SrTiO_3(001)$ surface remains an open question. Several periodic reconstructions have been experimentally observed and a few of these have been structurally solved [4,5]. Among these, the 2×1 reconstruction presents some interesting traits. Solved via a combination of transmission electron diffraction, direct methods and density functional theory [6], it exhibits two surface TiO_2 layers and a distinctive "dangling" oxygen atom in single coordination, as shown in Fig. 1(a). More importantly, but related to this, the 2×1 surface is predicted to have a much higher predicted surface energy (by >0.5 J/m²) relative to structures of the same stoichiometry [7], some of which have never been experimentally observed. Such thermodynamic instability is arguably too large to be overcome by kinetics alone; this remains an unresolved conundrum.

The interaction of $SrTiO_3(001)$ surfaces with water has been the subject of several studies, both experimental [8–11] and theoretical [12,13]. This is warranted, as H_2O in the vapor phase is truly

ubiquitous, making it very difficult to avoid said interaction; even in ultra-high vacuum environments, the presence of some residual water vapor is often unavoidable.

It is worth noting that light atoms, especially hydrogen, are exceedingly easy to miss when using diffraction techniques to decipher atomic structures. The possibility remains that certain surface reconstructions which have been declared structurally solved are, in fact, not dry. It has already been shown, for example, that the 2×2 and $(\sqrt{3} \times \sqrt{3})$ - $R30^{\circ}$ reconstructions of both MgO(111) and NiO(111) are hydroxylated [14,15]. On the SrTiO₃(001) surface, the high-energy 2×1 reconstruction is naturally a prime candidate for this.

The present report is the first of a two-part analysis of the SrTiO $_3$ (001) surface where we include the possibility of water chemisorption and what effect this has upon both the interpretation of existing STM images (this manuscript) and the overall energetics (the companion manuscript). Here, more specifically, we revisit scanning tunneling microscopy (STM) images of the 2×1 -reconstructed surface and of a surface structure with $c(4\times 4)$ periodicity which has not been structurally solved. By comparing the experimental micrographs to STM image simulations, we find strong evidence that the 2×1 reconstruction in the available STM data is in fact hydroxylated, and a partial dehydration results in the $c(4\times 4)$ surface. Not only does this provide a viable explanation of the data and how the $c(4\times 4)$ was obtained experimentally from the 2×1 , it is also consistent with the overall energetics of the surface (which we will postpone to the second part).

2. Methods

Density functional theory (DFT) calculations were performed for several surface structures using the full-electron-potential WIEN2k

^{*} Corresponding author: Tel.: +1 847 491 7809; fax: +1 847 481 7820. E-mail address: andres@u.northwestern.edu (A.E. Becerra-Toledo).

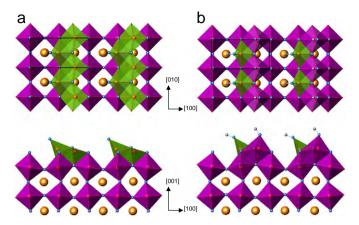


Fig. 1. Polyhedral representation of (a) the bare 2×1 reconstruction and (b) the hydrated 2×1 DissA model: plan view (top) and profile view (bottom). Surface cells outlined. Sr = large orange, Ti = red, O = blue, and H = gray. All polyhedra are Ti-centered and are green in 5-fold coordination and purple in 6-fold coordination.

code [16] with the augmented plane wave + local orbital (APW + lo) implementation. Each structure was modeled with the repeated slab configuration and relaxed until the residual force on each atom was below 0.1 eV/Å. The PBE [17] form of the generalized gradient approximation to the exchange-correlation functional was employed.

Surface slabs of 2×1 periodicity consisted of 13 atomic layers, plus any adsorbed atoms; slabs of $c(4\times4)$ periodicity, due to the additional computation expense, only have 9 atomic layers, plus the corresponding adsorbates. In order to compare total energy calculations, the 2×1 surfaces were also modeled with 9 atomic layers. Muffin-tin radii of 2.36, 1.70, 1.20 and 0.60 bohr were used for Sr, Ti, O and H, respectively. A k-point mesh equivalent to a $6\times6\times6$ mesh for a bulk SrTiO3 unit cell was used, as well as a $K_{\rm max}$ value of 5.5/1.2 bohr $^{-1}$. The SrTiO3 lattice parameter was optimized and a value of 3.944 Å (1% larger than the experimental figure) was used. High-bias, constant-current scanning tunneling micrographs were simulated using the DFT outputs via a modified Tersoff–Hamann approach, as outlined in detail elsewhere [18]; a more concise description follows below.

After allowing a structure to relax and reach full charge density convergence, the unoccupied states up to $E_{\rm F}+eV_{\rm b}$ are artificially populated, with the regular population multiplied by a weighting factor proportional to $\kappa(\varepsilon)^{-2}$. Here, $\kappa(\varepsilon)=\hbar^{-1}\sqrt{2m_{\rm e}(\phi_{\rm t}+eV_{\rm b}+E_{\rm F}-\varepsilon)}$ is the inverse decay length of the electron states in vacuum for energy ε , $E_{\rm F}$ is the Fermi energy of the sample, $V_{\rm b}$ is the bias voltage, $\Phi_{\rm t}$ is the tip work function, $m_{\rm e}$ is the mass of an electron and e is its charge. This accounts for the larger effective tunneling barrier observed by electrons tunneling elastically into surface states of lower energies.

The artificial density is sampled over a volume near the surface, with 0.2 Å in-plane and 0.3 Å out-of-plane sampling intervals, thereby generating a 3D array of densities. Blurring due to tip size, vibration and thermal effects was simulated by convolving the density at each voxel with an inplane radially-symmetric step-function motif. Upon specification of a density value, an isosurface of constant density was produced, analogous to the generation of a surface of constant current in experimental STM. Grayscale coloring, scaled with height at each in-plane position, was applied. The simulated STM image is thus a representation of the colored isosurface down the direction normal to the sample surface.

3. Results

Johnston et al. [19] reported constant-current scanning tunneling micrographs of the 2×1 -reconstructed SrTiO $_3$ (001) surface. The images clearly resolve the 2-unit cell periodicity, but not the

perpendicular single-cell period, so the surface appears as rows: a typical experimental STM image of the 2×1 surface is shown in Fig. 2(a). The average row height is plotted in Fig. 2(b) as a function of position along the 2-unit cell periodicity direction with a typical corrugation height of between 0.4 and 0.5 Å.

In order to test structural models by simulating constant-current STM image simulations, DFT calculations were carried out for two structures: the bare 2×1 structure proposed by Erdman et al. [6]; and the 2×1 DissA model, which adds one dissociatively-adsorbed H_2O molecule per 2×1 cell, and is the lowest energy model among several adsorption geometries (see Part II for more details). Model 2×1 DissA is shown in Fig. 1(b) and adds an OH group on the most undercoordinated surface Ti as well as a lone H terminating each "dangling" O. For the STM simulation of each structure, the density was set so as to match the average corrugation above, fixed at 0.45 Å. The corresponding images are shown in Fig. 3(a) and (b).

As can be seen, neither image successfully reproduces the experimental micrograph or the average row height plot. While in the bare 2×1 simulation the characteristic dangling O dominates the image, in 2×1 DissA it is the adsorbed OH group that is the most salient feature. As we relax the strict average height constraint, changing the specified isosurface density produces simulations that are closer to the experiment. An isosurface at a lower density leads to the dry 2×1 qualitatively matching well with the image itself, although the average height curve shape is too broad and the corrugation necessary is 0.29 Å; see Fig. 3(c). On the other hand, the 2×1 DissA model also matches well with the image, but does reproduce very successfully the sinusoidal average height curve, as can be seen in Fig. 3(d); even the relative sharpness of the troughs, compared to the peaks, is discernible in the simulation. In this case, the average corrugation was 0.49 Å, which is within the observed experimental range.

These results strongly suggest that the 2×1 structure contains H_2O , but there is some ambiguity so more evidence is needed to be unconditional, and this comes from a second structure, a $c(4\times4)$ reconstruction.

A report by the same research group [20] describes the gradual generation of a $c(4\times4)$ reconstruction upon UHV annealing (starting at 900 °C) of a SrTiO₃(001) sample with a pre-existing 2×1 surface reconstruction, previously formed at 600-800 °C. The $c(4\times4)$ reconstruction appears in the STM micrograph as a distinctive "brickwork" pattern of short linear units, as seen in Fig. 4, and should not be confused with the two "square" reconstructions, also of $c(4\times4)$ periodicity, observed by Kubo and Nozoye [21]. Similar to the 2×1 surface, the "brickwork" arrangement was also found in domains with two perpendicular orientations. This suggests the possibility of the $c(4\times4)$ and 2×1 being structurally similar, except for the presence of different amounts of adsorbed H_2O . In such a scenario, the change would be due to the partial desorption of H_2O , and ordering of the remaining adsorbates. Naturally, this would imply that the 2×1 is hydrated.

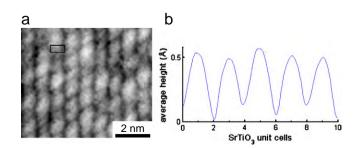


Fig. 2. (a) Scanning tunneling micrograph of the 2×1 -reconstructed surface, with unit cell outlined; 2.0 V bias voltage, 0.5 nA tunneling current. (b) Typical average height plot, upon averaging along the rows.

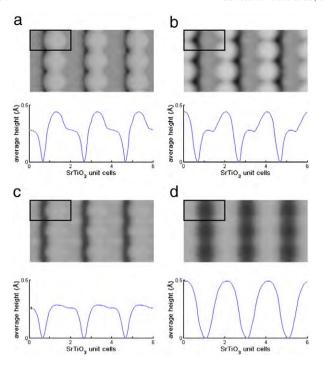


Fig. 3. Simulated STM micrograph at 2.0 V bias voltage (top) and average row height plot (bottom) of (a, c) the bare 2×1 reconstruction and (b, d) the 2×1 DissA model. Panels (a, b) result from the constraint of fixing the average row corrugation to 0.45 Å. Panels (c, d) are the best matching simulations upon relaxing said constraint.

Two $c(4\times4)$ models based on an underlying bare 2×1 structure were constructed, both with two dissociatively-adsorbed H₂O molecules per $c(4\times4)$ cell, following the favored adsorption sites of the 2×1 DissA model, which has twice as much adsorbed water. These models are shown in Fig. 5.

 $c(4\times4)A$: The adsorbed OH pair up, with each pair member being one bulk unit cell away from its partner. The lone H are evenly spread out, each one sitting roughly halfway between two OH pairs. The structure is available as Supplementary material in the Crystallographic Information File (CIF) format.

 $c(4\times4)B$: This model is based on a different orientation of the underlying 2×1 , perpendicular to the one used in the first model. The adsorbed OH are evenly spread out, each of them two unit cells away from the closest such units. The lone H pair up, with each pair joining two adsorbed OH groups to form a large unit which could potentially give rise to the characteristic linear

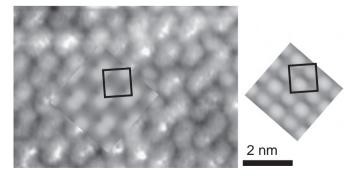


Fig. 4. (Left) Experimental scanning tunneling micrograph of the surface exhibiting an almost fully-ordered "brickwork" $c(4\times4)$ surface structure; 2.0 V bias, 10 nA current. Simulated 2.0 V STM image for the $c(4\times4)$ A model is superposed, with the surface cell outlined. (Right) Simulated 2.0 V STM image for the $c(4\times4)$ B model.

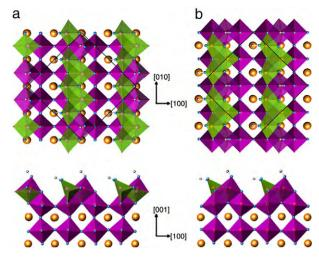


Fig. 5. Polyhedral representation of (a) the $c(4\times4)A$ model and (b) the $c(4\times4)B$ model: plan view (top) and profile view (bottom). Surface cells outlined.

feature seen in STM. This structure is also available as Supplementary material in CIF format.

The corresponding DFT-based STM micrograph simulations (bias voltage of $2.0\,\text{V}$) are shown in Fig. 4. It is clear that model $c(4\times4)B$ can be easily discarded, as the individual OH units dominate the image. However, the simulation for the $c(4\times4)A$ model, superposed to the experimental image in Fig. 4, is highly successful. Each pair of adsorbed OH forms a single linear STM feature, of comparable size to what is observed experimentally.

Moreover, total energy calculations show that not only is $c(4\times4)A$ more thermodynamically stable than $c(4\times4)B$, but it also has a slightly lower energy than the average of the dry 2×1 and the 2×1 DissA model; these results are presented in Part II.

4. Discussion

The DFT-based simulations of scanning tunneling micrographs support the idea that the 2×1 surface reconstruction carries dissociatively-adsorbed water at least sometimes, if not always. For the dry 2×1 model, no choice of isosurface density yields a satisfactory match to the experimental data. The average height curve fails to mimic the measured curve, with its shape only vaguely approaching the observed sinusoidal nature at densities with which the average corrugation is too small. The hydroxylated 2×1 DissA model is a better match, as the predicted average corrugation does not decay as fast with density. As seen in Fig. 3(d), it is possible to find a range of densities in which the image, average corrugation and sinusoidal height curve shape are reproduced faithfully.

Moreover, the examination of hydroxylated 2×1 -based models for the brickwork $c(4\times4)$ reconstruction (at present unsolved, structurally) supports the previous finding by explaining the 2×1 -to $c(4\times4)$ transition as a simple dehydration process. The structural models analyzed are both (stoichiometrically) halfway between the dry and hydrated 2×1 models above. The main difference lies in the position of the adsorbed OH groups, which dominate the simulated STM micrographs. In the $c(4\times4)A$ model, they pair up and within each pair the OH-OH in-plane distance is roughly one bulk unit cell; in the $c(4 \times 4)B$ model, they are spread out, qualitatively forming a 2×2 periodicity. It is evident from the simulations that a 2×1 -based $c(4\times4)$ model requires the former hydroxyl arrangement to reproduce the observed linear STM features. As for the lone adsorbed H atoms, their exact position is hard to decipher, since their presence is shadowed in the simulated micrographs by the adsorbed OH groups; it is to be expected that each lone H will bind to a dangling

O, however. While it is straightforward to come up with a structure that differs from the $c(4\times4)A$ only in the arrangement of these lone H, the adsorption sites chosen above do appear to yield a good match to the less bright regions of the experimental image.

Of course there are inherent limitations in comparing STM image simulations with experimental data, which tends to be restricted to qualitative evaluation. One of the main issues is that tip-sample interactions are not accounted for in our simulations, and this can be particularly relevant for surfaces with adsorbed molecules that are easily moved by the STM tip, such as dangling OH groups. Nevertheless, the significant differences in the simulated images presented herein and the good match of only one of the 2×1 and one of the $c(4\times4)$ simulations to the experiments allow us to be confident that we have identified the correct structures.

As shall be seen more quantitatively in terms of bond valence sums in Part II, the characteristic dangling O is not the only undercoordinated atom in the bare 2×1 surface model. The top-layer Ti not bound to the dangling O is 5-fold coordinated, but due to the coordination of the four top-layer O it is bound to, every Ti-O bond length is constrained. As a result, that Ti is quite exposed and is not very stable. It is no coincidence that these two atoms (the dangling O and the exposed surface Ti) are the preferred adsorption sites for dissociated water. Each of the two sites is quantifiably much more stable upon the adsorption of H or OH. This conclusion solves the question of the instability of the previously accepted, dry 2×1 structural solution; whether a stable, dry 2×1 reconstruction could form in the absence of any water vapor is an open question, but it appears unlikely, considering the energetic constraints.

In the case of the experimental STM report of the 2×1 reconstruction, the sample was prepared by following the recipe by Kawasaki et al. [22] which results in the chemical etching of surface SrO, leaving TiO₂-terminated surfaces only. Said recipe calls for a bath in a buffered NH₄F-HF solution, followed by rinsing in water and drying with N2 gas. It is known that carbonaceous surface contamination occurs, and it is hard to envision all H₂O (or hydroxyl groups) being removed, especially if there are surface defects present; it is well known that defective SrTiO₃(001) surfaces favor strong dissociative adsorption [9-11]. The same is true for samples prepared via ion sputtering. We will return to this point later in Part II.

5. Conclusions

We have shown via DFT-based simulations that the experimental STM images of the SrTiO₃(001) 2×1 surface reconstruction are more consistent with a structural model that differs from the presently accepted model by the addition of one dissociatively-adsorbed H₂O molecule per 2×1 cell. Additionally, we have explained the 2×1 -to $c(4\times4)$ transition upon annealing as a simple dehydration mechanism, by using the new 2×1 structural model as the starting surface and examining $c(4\times4)$ models based on it. We propose one of these as the structural solution to the $c(4\times4)$ surface reconstruction, given the striking agreement of its simulated STM micrograph to the experimental data.

Supplementary materials related to this article can be found online at doi:10.1016/j.susc.2012.01.008.

Acknowledgments

We thank Prof. K.R. Poeppelmeier for useful discussions. This research was supported by the U.S. Department of Energy, under award number DE-FG02-01ER45945, and by the National Science Foundation, under award number DMR-0906306. The authors acknowledge that the research reported in this study was in part performed on Quest, Northwestern University's centrally provided high performance computing facility, which is operated by Northwestern University Information Technology. Use of the Carbon Cluster at the Center for Nanoscale Materials was supported by the U.S. Department of Energy, Office of Science, Office of Basic Energy Sciences, under award number DE-AC02-06CH11357.

References

- [1] X.D. Qi, M. Wei, Y. Lin, Q.X. Jia, D. Zhi, J. Dho, M.G. Blamire, J.L. MacManus-Driscoll, Appl. Phys. Lett. 86 (2005) 071913.
- A. Kudo, Y. Miseki, Chem. Soc. Rev. 38 (2009) 253.
- A.F. Santander-Syro, O. Copie, T. Kondo, F. Fortuna, S. Pailhes, R. Weht, X.G. Qiu, F. Bertran, A. Nicolaou, A. Taleb-Ibrahimi, P. Le Fevre, G. Herranz, M. Bibes, N. Reyren, Y. Apertet, P. Lecoeur, A. Barthelemy, M.J. Rozenberg, Nature 469 (2011) 189.
- N. Erdman, O. Warschkow, M. Asta, K.R. Poeppelmeier, D.R. Ellis, L.D. Marks, J. Am. Chem. Soc. 125 (2003) 10050.
- R. Herger, P.R. Willmott, O. Bunk, C.M. Schlepütz, B.D. Patterson, Phys. Rev. Lett. 98 (2007) 076102.
- N. Erdman, K.R. Poeppelmeier, M. Asta, O. Warschkow, D.R. Ellis, L.D. Marks, Nature 419 (2002) 55.
- O. Warschkow, M. Asta, N. Erdman, K.R. Poeppelmeier, D.E. Ellis, L.D. Marks, Surf. Sci. 573 (2004) 446.
- C. Webb, M. Lichtensteiger, Surf. Sci. Lett. 107 (1981) L345.
- S. Eriksen, P.D. Naylor, R.G. Egdell, Spectrochim. Acta A 43 (1987) 1535.
- N.B. Brookes, F.M. Quinn, G. Thornton, Vacuum 38 (1988) 405.
- L.-Q. Wang, K.F. Ferris, G.S. Herman, J. Vac. Sci. Technol. A 20 (2002) 239.
- R.A. Evarestov, A.V. Bandura, V.E. Alexandrov, Surf. Sci. 601 (2007) 1844.
- B.B. Hinojosa, T. Van Cleve, A. Asthagiri, Mol. Simul. 36 (2010) 604.
- J. Ciston, A. Subramanian, L.D. Marks, Phys. Rev. B 79 (2009) 085421 J. Ciston, A. Subramanian, D.M. Kienzle, L.D. Marks, Surf. Sci. 604 (2010) 155.
- P. Blaha, K. Schwarz, G.K.H. Madsen, D. Kvasnicka, J. Luitz, WIEN2k, an Augmented
- Plane Wave + Local Orbitals Program for Calculating Crystal Properties, Universität Wien, Austria, 2010
- [17] J.P. Perdew, K. Burke, M. Ernzerhof, Phys. Rev. Lett. 77 (1996) 3865.
- A.E. Becerra-Toledo, M.S.J. Marshall, M.R. Castell, L.D. Marks, submitted for publication.
- K. Johnston, M.R. Castell, A.T. Paxton, M.W. Finnis, Phys. Rev. B 70 (2004) 085415.
- M.R. Castell, Surf. Sci. 505 (2002) 1.
- T. Kubo, H. Nozoye, Surf. Sci. 542 (2003) 177.
- [22] M. Kawasaki, A. Ohtomo, T. Arakane, K. Takahashi, M. Yoshimoto, H. Koinuma, Appl. Surf. Sci. 107 (1996) 102.